AGU ADVANCING EARTH AND SPACE SCIENCE

Water Resources Research

TECHNICAL REPORTS: METHODS
10.1029/2020WR028140

Key Points:
- Distributed acoustic sensing (DAS) can accurately measure dynamic bedrock strain at low frequency
- The distributed strain measurement identified fluid stimulation of hydraulically connected bedrock fractures
- Measurement of hydromechanical response in wells provides a robust tool for establishing bedrock plumbing in groundwater and geothermal systems

Supporting Information:
- Supporting Information S1

Correspondence to:
M. W. Becker,
matt.becker@csulb.edu

Citation:
Becker, M. W., Coleman, T. I., & Ciervo, C. C. (2020). Distributed Acoustic Sensing as a Distributed Hydraulic Sensor in Fractured Bedrock. *Water Resources Research*, *56*, e2020WR028140. https://doi.org/10.1029/2020WR028140

Received 10 JUN 2020
Accepted 12 AUG 2020
Accepted article online 14 AUG 2020

Distributed Acoustic Sensing as a Distributed Hydraulic Sensor in Fractured Bedrock

M. W. Becker[1], T. I. Coleman[2], and C. C. Ciervo[1]

[1]Department of Geological Sciences, California State University Long Beach, Long Beach, CA, USA, [2]Silixa LLC, Missoula, MT, USA

Abstract Distributed acoustic sensing (DAS) was originally intended to measure oscillatory strain at frequencies of 1 Hz or more on a fiber optic cable. Recently, measurements at much lower frequencies have opened the possibility of using DAS as a dynamic strain sensor in boreholes. A fiber optic cable mechanically coupled to a geologic formation will strain in response to hydraulic stresses in pores and fractures. A DAS interrogator can measure dynamic strain in the borehole, which can be related to fluid pressure through the mechanical compliance properties of the formation. Because DAS makes distributed measurements, it is capable of both locating hydraulically active features and quantifying the fluid pressure in the formation. We present field experiments in which a fiber optic cable was mechanically coupled to two crystalline rock boreholes. The formation was stressed hydraulically at another well using alternating injection and pumping. The DAS instrument measured oscillating strain at the location of a fracture zone known to be hydraulically active. Rock displacements of less than 1 nm were measured. Laboratory experiments confirm that displacement is measured correctly. These results suggest that fiber optic cable embedded in geologic formations may be used to map hydraulic connections in three-dimensional fracture networks. A great advantage of this approach is that strain, an indirect measure of hydraulic stress, can be measured without beforehand knowledge of flowing fractures that intersect boreholes. The technology has obvious applications in water resources, geothermal energy, CO_2 sequestration, and remediation of groundwater in fractured bedrock.

Plain Language Summary A technology developed for measuring vibrations on fiber optic cable, distributed acoustic sensing, is used to measure strain in bedrock in response to pumping and injection. This technology is extremely sensitive to dynamic strain, measuring displacements approaching the size of a water molecule. Field tests showed that fluid-induced strain in rock exhibits complex geometry. The technology can be used to better understand flow in bedrock, optimize geothermal energy extraction, and identify leakage from subsurface injection systems.

1. Introduction

A hallmark of fractured rock hydrology is complex three-dimensional flow behavior (National Academies of Sciences and Medicine, 2015). Unlike alluvial systems which tend to be hydrostratigraphic, fracture orientations in crystalline bedrock are dictated primarily by the stress field, which can create unpredictable hydraulic interconnectivity. Fractured-rock hydrologists have long referred to the "plumbing" of bedrock systems because water can be channeled in unexpected directions (National Research Council, 1996). To understand bedrock plumbing, hydraulic responses to pumping or injection are observed using boreholes that are isolated over discrete intervals, typically with inflatable bladders (packers). The challenge with the current state of hydraulic characterization of fracture bedrock is that monitoring requires prior knowledge of the connections to be isolated. Often, borehole geophysics is used to find fractures, and the permeabilities of these fractures are estimated with active or passive flow logging. By iteratively applying logging and packing in multiple boreholes, the plumbing of the formation can be characterized, but this process is time-consuming, expensive, and limited by the poor resolution of borehole flow meters (Paillet, 1993). Chemical or thermal tracers can be used, but tracer breakthrough can be prohibitively slow and usually does not result in identification of specific flow zones. Thermal tracers combined with fiber optic distributed temperature sensing may lead to such detailed flow mapping (Klepikova et al., 2014), but this approach is feasible only for closely spaced wells due to tracer heat dissipation.

Here we develop a "distributed" hydraulic sensor that circumvents the need to predetermine the fracture connectivity of a formation to establish its hydraulic connectivity. Rather than measure pressure directly, fracture strain in response to hydraulic stress is measured. Strain is used instead of stress because it can be measured using a relatively new fiber optic sensing technology called "Distributed Acoustic Sensing" or DAS. By mechanically coupling the fiber to the formation, strain in response to hydraulic pressure propagation can be measured with extremely high precision. This is an indirect measure of pressure. Fracture compliance must be known to make the transformation from measured rock strain to fluid pressure. However, the timing of pressure propagation (e.g., hydraulic diffusivity) is often more important than magnitude to understand hydraulic connectivity in bedrock systems (Illman et al., 2009).

Fiber optic sensing technology has multiple advantages over traditional pressure transducer measurements. Distributed sensing results in an effective measurement "array" along the length of the fiber with a density of meters or less. Fiber optic distributed measurements can be kilometers long, and fiber optic cabling can be constructed to withstand adverse pressure, temperature, and chemical environments (Schenato, 2017). Fiber optic cable is relatively inexpensive, so it can be installed sacrificially in a borehole either cemented outside of casing or in a dedicated slimhole (Becker et al., 2018a). The possibility of fluid movement along borehole, which could lead to blended hydraulic head measurements or cross-contamination, is avoided by cementing the fiber into boreholes. Finally, the same cable can be used to simultaneously measure temperature with fiber optic distributed temperature sensing.

In this article we describe pilot field experiments conducted in a bedrock well field. DAS was used to measure fracture displacement in two boreholes in response to periodic pumping and injection at another borehole in the field. Laboratory experiments were conducted to demonstrate that displacement measurements are reliable and to assess the spatial resolution of the method. This article follows a previous article (Becker, Ciervo, et al., 2017) in which we demonstrated that time-series geomechanical responses correlate with measure fluid pressure in one of the boreholes. In the current article, we demonstrate the spatial rather than the temporal resolution of the method. Specifically, we demonstrate how DAS can locate hydraulically conductive fractures by measuring the fracture displacement in response to fluid pressure in two separate boreholes.

1.1. Distributed Acoustic Sensing

The principles of DAS are well documented in the published literature (Hartog, 2017; Parker et al., 2014). The system consists of a fiber optic cable, usually with single mode fiber, connected to an interrogator unit. The interrogator used in this study employs phase demodulation of a laser backscatter signal to measure displacement rate along the cable (phase optical time domain reflectometry or Φ-OTDR). This is accomplished over a specified gauge length (e.g., 10 m), so strain rate is calculated as measured displacement rate divided by the gauge length. Time of photon flight is used to position the signal along the cable. In the experiments reported here, a measurement was collected every 0.25 m along the cable. Typically, temporal sampling is made at a frequency of 1 kHz or greater to sample vibrations of frequencies between hertz and kilohertz. The dynamic range of DAS extends from kilohertz to microhertz (Becker & Coleman, 2019; Lindsey et al., 2020). Because of the native measurement displacement rate, signal-to-noise degrades at lower frequencies. In the experiments reported here, fiber displacement of less than 1 nm was measured at millihertz frequencies (Becker, Coleman, et al., 2017).

The key to measuring strain in a bedrock borehole is to couple the fiber mechanically to the borehole wall. For horizontal boreholes, the coupling is surprisingly good from just friction (Richter et al., 2019). For vertical boreholes, the fiber must be either grouted into the borehole or pressed against the borehole wall. Grouting or cementing the fiber outside of the casing provides the most robust coupling (Correa et al., 2019), although clamping systems have also been designed (Daley et al., 2015). For shallow applications, a pressured flexible liner may be used to temporarily couple the fiber against the borehole wall (Becker, Ciervo, et al., 2017; Munn et al., 2017).

Even when the fiber optic cable is coupled to the formation, strain may not be perfectly transferred through the cable itself (Becker et al., 2018b; Lindsey et al., 2020). Downhole cables are generally designed to limit strain on the fiber to prevent damage. Structures that are designed to prevent fluids from contacting the optical fiber also limit strain transfer. For example, fiber-in-metal tube (FIMT) constructions are typically used

where the fiber is contained within a continuous single- or double-walled stainless-steel tube, and a hydrogen scavaging gel surrounds the fiber to help prevent hydrogen darkening. As a result, fiber optic cable construction can have a marked impact on strain measurement. For example, Becker et al. (2018b) cemented five different cables of varying design into a single PVC pipe and then strained that pipe using a stepper motor. DAS measured strains in the fibers varied by a factor of two, even though they were all subjected to identical displacement.

Applications of DAS technology have been explored most thoroughly for oil and gas applications (Cannon & Aminzadeh, 2013; Li et al., 2015). More recently, it has been adopted for monitoring geothermal reservoirs where the temperature resistance of cables holds a unique advantage over electronic sensors (Paulsson et al., 2014). The most common application of DAS is to use the fiber as an array of geophones for seismic applications. These may be downhole observations as previously noted or, most recently, in using unused or "dark" fiber in existing communications networks to observe ground motions (Jousset et al., 2018; Lindsey et al., 2017). The potential for hydrologic applications has been recognized recently in the literature (Munn et al., 2017; Schenato, 2017). Although seismic velocity can be used to measure properties of interest to hydrology, such as depth to water table or soil moisture (Ajo-Franklin et al., 2017), the focus here is on using DAS as a dynamic strain meter.

2. Materials and Methods

2.1. Laboratory Tests

To confirm that DAS can correctly measure strain, a series of laboratory experiments were carried out using the iDAS™, manufactured by Silixa (Elstree, Hertfordshire, UK, www.silixa.com). A 900 μm OD tight buffered 9/125 μm single-mode fiber was chosen for this experiment as it most closely resembles a "bare" fiber unaffected by cabling. The fiber was epoxied into half-inch PVC sections which were mounted into aluminum brackets (supporting information Figure S1). The length of fiber between the two mounts was 30 mm. Two synchronized linear actuator stepper motors (Anaheim Automation, Model 17AW102Px06-LW4-EL) were used to drive the separation of plates. These motors have 200 steps per revolution and move 3.969 micron per step. However, using a stepper driver (Applied Motion, ST10-Si) it is possible to move the motor 51,200 microsteps per revolution, resulting in a fiber displacement of 15.5 nm/microstep. The motor was programmed to approximate a sinusoidal displacement with a period of 6.9 seconds and a displacement amplitude that varied between 17.5 and 40 μm. These amplitudes were much larger than those measured in the field but were chosen such that displacement could be independently verified using a caliper.

The Silixa iDAS instrument was set with a temporal sampling rate of 1 kHz, a spatial sampling of 0.25 m, a laser repetition rate of 50 kHz. Raw DAS output files were converted to displacement rate (nm/s) using a Matlab® algorithm provided by the vendor. Displacement rates were converted to displacement by integrating the time series using the cumtrapz function in Matlab®. Although the displacements applied to the fiber were large, the iDAS measures displacement rate natively. Consequently, there were no issues with signal clipping of the data due to large fiber displacement.

To extract the amplitude of displacement, three alternative methods were tested. First, amplitudes of the displacement signal were extracted using the peak at the known dominant frequency from a Fast Fourier Transform (FFT). A flattop window correction was applied to account for peak frequencies that fell near bin edges (Lyons, 2011). Second, the same approach was used on the displacement rate signal, but the result was converted to displacement using the equivalent analytic solution for an integrated sine function, that is, dividing by $2\pi f$, where f is the frequency of oscillation. Third, an envelope approach was used in which a running maximum and minimum of the signal were differenced and halved to find the amplitude. An averaging window of 125% of the signal period appeared to work best. No filtering or other processing was applied in any of the three approaches.

2.2. Field Tests

Field tests were conducted at the Mirror Lake Fractured Rock Hydrology site, New Hampshire, USA, within the Hubbard Brook Experimental Forest. The Mirror Lake site was established by the U.S. Geological Survey's Toxic Substances Hydrology program to investigate contamination issues in fractured bedrock (Hsieh & Shapiro, 1996). The site itself is free of any contamination, and the wells are on U.S.

Forest Service property. The many prior investigations conducted in the Forest Service East (FSE) well field (Figure S2) provided an important baseline for the hydraulic studies conducted for this work (Shapiro et al., 1995). Bedrock at the FSE well field is composed primarily of granitoids that have intruded the peletic schist country rock (Johnson & Dunstan, 1998). A combination of tectonic and unloading stresses has resulted in a complex fracture network throughout the crystalline bedrock to a depth of at least 300 m. Individual fractures tend to extend less than 10 m in length, so permeability and transport are along interconnected fractures and fracture zones (Ellefsen et al., 1998; Hsieh & Shapiro, 1996; Shapiro, 2001). There is no measurable permeability in the rock matrix; groundwater moves through sparse networks of interconnected fractures with length of about 5–10 m (Barton et al., 1997). Previous DAS experiments in this well field resulted in fracture compliance estimates between 4.3e-11 and 1.9e-12 m/Pa (Becker, Ciervo, et al., 2017).

To conduct periodic hydraulic tests, FSE 6 (Figure S2) was subjected to alternating pumping and injection to create either periodic step or approximately sinusoidal hydraulic signals, which result in periodic strain in the formation (Schuite et al., 2017). This was accomplished using two variable speed pumps (Grundfos RediFlo2) controlled by two programmable variable speed controllers. Rasmussen et al. (2003) used a similar setup to conduct periodic hydraulic tests in unconsolidated sediments. A tank located near the wellhead was used to store water for reinjection. Flow meters uphole and downhole were used to assure that the injection and pumping rates were kept equivalent during the tests. For the results discussed here, periodic step tests were used. In the periodic step tests, pumping and injection were alternated at a constant rate of about 15 L/min (Becker et al., 2016). Periodic step tests were conducted with oscillation periods of 2, 4, 8, 12, and 18 minutes, with the first half-period pumping and the second half-period injecting. During the oscillation of flow in FSE 6, heads were recorded in FSE 6 and the five monitoring wells using pressure transducers. The difference between maximum and minimum head in FSE 6 ranged from about 2 m for the short period (2 min) tests to about 7 m for the long period (18 min) tests.

In FSE9 and FSE10, fiber optic cable was mechanically coupled to the borehole wall using an overpressured flexible (FLUTe™) liner used also by Munn et al. (2017) for seismic (VSP) DAS monitoring. These liners were originally developed to prevent cross-connection and allow discrete-level monitoring in bedrock wells (Cherry et al., 2007). The liner is made from an impermeable, tubular, flexible nylon fabric that extends from the top of the well (anchored at the well casing) into the borehole. During installation, about 3 m of overpressure head is maintained to evert the liner down the well and simultaneously couple the FO cable to the borehole wall past the target fracture depth. The overpressure head in the liner was more than an order-of-magnitude greater than any head response from oscillatory pumping tests in the well, ensuring that the FO cable remains coupled to the rock wall. In FSE 10, the liner was fitted with a permeable mesh woven into the fabric at the depth of the transmissive fractures known from previous studies (28 m). A pressure transducer at the surface was connected to a tube in communication with the permeable mesh (Becker, Ciervo, et al., 2017). Because the tube is filled with both water and air, pressure transducer measurements had to be compensated for compression of air in the tubing (Keller, 2016). The liner was reused, and the tests repeated for FSE 9, but pressure could not be measured simultaneously because the transducer port was not correctly located. A comparison between fluid pressure and displacement at the fracture horizon in FSE 10 was reported previously (Becker, Ciervo, et al., 2017).

Fiber optic cables designed specifically for strain sensing were deployed in both FSE 9 and FSE 10. In this strain transfer optimized construction, the optical fiber is surrounded by a solid filling material within the FIMT rather than gel. Gel-filled FIMT constructions are common in downhole applications but reduce the strain sensitivity by hampering strain transfer from the outer cable jacket to the glass fiber. Gel-filled FIMT designs can have about half of the strain sensitivity of some strain transfer optimized designs such as tactical tight-buffered cables as has been discussed elsewhere (Becker et al., 2018a).

Changes in temperature can cause fiber strain and interfere with mechanical strain measurements. Temperature was monitored during the tests using Distributed Temperature Sensing (DTS). A Silixa Ultima-S instrument (Elstree, Hertfordshire, UK, http://www.silixa.com) with an expected precision of 0.01 C collected temperature every 30 minutes at each 12.6 cm along the entire fiber network. No measurable temperature changes occurred in the monitoring wells during the experiment. In any case, because we are extracting periodic strain measurements changes in temperature would have resulted only in a trend or drift in the dynamic strain measurements, amplitude measurements would not be affected.

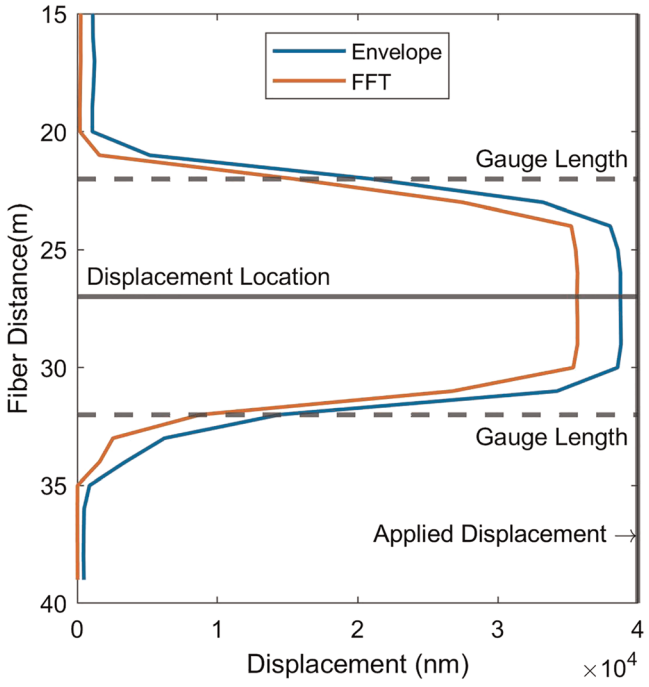

Figure 1. Effect of gauge length on the measurement of 40,000 nm of displacement on a fiber stretched at distance 27 m along the fiber. The measurement window width equal to the gauge length is shown about the known location of displacement.

Because our target frequency in the megahertz range, we down-sampled the 1,000 Hz sampling rate to 100 Hz using the Matlab "decimate" command which applies a lowpass Chebyshev Type I infinite impulse response (IIR) anti-aliasing filter of order 8. Decimated data are available on the Department of Energy Geothermal Data Repository (Becker & Coleman, 2017). This reduced file size and processing time without affecting signal quality. Displacement amplitudes were extracted from the signals using the min/max enveloping method which provided the best measurement of displacement in the laboratory tests (section 3.1 and Supplemental Matlab Script). Displacement amplitudes were extracted for each channel within the wellbore. The depth to the water level in the borehole liner proved to be a reliable signal to allow channels to be depth-correlated. It is worth noting that in previous analysis of amplitudes (Becker et al., 2018a; Becker, Ciervo, et al., 2017), we used a recursive leaky filter to integrate displacement rate to find displacement. This approach proved to produce erroneous displacement measurements. The laboratory experiments discussed above demonstrated that this method, which seems to be sufficient for higher frequency signals, underestimated strain amplitudes by nearly an order-of-magnitude.

3. Results

3.1. Laboratory Tests

The amplitude of displacement measured by DAS is regressed against displacement induced by the stepper motor. This amplitude was determined from the min/max enveloping approach described above. Even with correction for scalloping, both FFT methods underpredicted the induced amplitudes with a regression slope of about 0.85, so were not used further. Figure 1 illustrates the difference in amplitude measured using the FFT applied to the integrated displacement rate and the min/max envelope applied to the same data. Using the min/max enveloping of the integrated displacement rate, the slope of the regression is near 1, while the coefficient of determination (R^2) indicates excellent agreement between the DAS measured displacement and the actual displacement induced by the stepper motor, which was confirmed with a caliper. The tests indicate that, under ideal conditions, the DAS instrument is capable of accurately measuring displacement. Strain is obtained by dividing displacement by the gauge length of 10 m.

The iDAS measures the dynamic interference of photons returned from positions on the fiber optic cable separated by a gauge length (Hartog, 2017). Displacement is recorded at the channel centered between these gauge positions. A point displacement on the fiber will, therefore, be sensed within a moving measurement window with a width equal to the gauge length. This windowing is illustrated in Figure 1, which shows the displacement measured at each channel (recorded at every 0.25 m) surrounding the stretched fiber location at position 27 m. Although the stepper motor stretched only 3 cm of fiber, the displacement is sensed over a 10 m distance equal to the gauge length. Multiple displacement signals cannot be separated within a gauge length, but a single displacement can be located at the center of this displacement signal.

DAS measurements slightly underpredict induced displacement at the largest displacements. The reason for this is not known. The maximum displacement applied to the fiber in these experiments was 40 microns over a 3 cm length of fiber or 0.133% strain. The maximum displacement is well below the breaking point of the fiber (0.5% strain) but may have resulted in some change in the optical properties of the glass. It may also be that the stepper apparatus is not perfectly rigid, and there is some slippage or deflection of the various parts. It is important to realize that these induced fiber displacements were very large to allow them to be controlled by the stepper motor. Laboratory displacements were four orders-of-magnitude larger than those measured in the field experiments. Consequently, we expect linearity between mechanical and DAS-measured displacements in the field experiments.

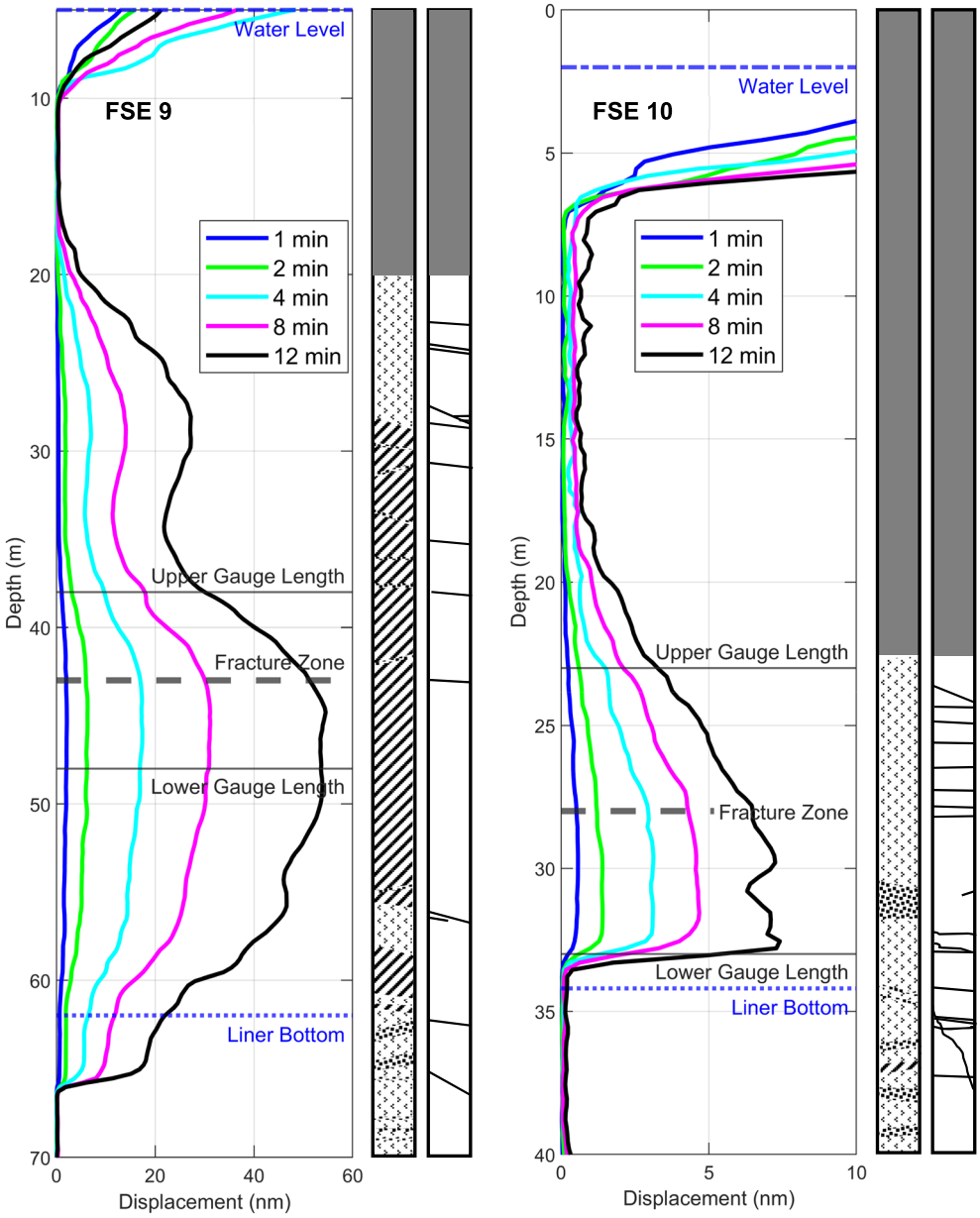

Figure 2. DAS displacement amplitude for five pumping periods (colored coded) measured along fiber optic cable anchored in FSE 9 (left) and FSE 10 (right). Fracture zones known a priori to be hydraulically communicating are indicated by dashed lines. Borehole lithologic and fracture logs are shown for comparison (after Johnson & Dunstan, 1998).

3.2. Field Tests

Repeating the alternating injection and pumping at FSE 6, with the same rate but with larger periods, resulted in an increased volume of water being injected in the formation. Increase in periodically injected water volume resulted in an increase in the hydraulic response at the observation wells, FSE 9 and FSE 10. The increased hydraulic response led to greater fracture dilation and, consequently, greater displacement in the fiber optic cable anchored to the borehole wall with the flexible liner. In a previous article (Becker, Ciervo, et al., 2017), hydraulic and displacement responses were compared in FSE 10 where a pressure transducer was installed. Here, the focus is on the displacement distribution surrounding the hydraulically stimulated fracture zone.

After integration through time to convert displacement rate (nm/sample) to displacement (nm), periodic strain responses are clearly visible in the DAS displacement matrix (Figure S3). Amplitudes are extracted through the enveloping method describe above and demonstrated in the Matlab® LiveScript® available as file "**ExampleProcessingDAS.mlx**" in the supporting information. Samples represent 0.01 second intervals (100 Hz sampling rate). Channels are responses along the fiber, measured in the center of the gauge length, which can be related to depth. Even with simple integration, the periodic strain behavior is seen clearly in the data. Strain is greatest at the depth of the connected fracture zone at 43 m depth in FSE 9, corresponding to channel 121. The strain signal is artificially extended through the channels by the gauge length of 10 m (40 channels). Notice that away from this zone the displacement response is delayed slightly as strain is transferred from the conductive fracture to the rock matrix.

Figure 2 shows the displacement amplitude measured at each recording channel in the two boreholes. Examples of the time-series displacement may be found in the supporting information and in a previous publication (Becker et al., 2016). Amplitudes were computed, using the enveloping method, for each channel recorded by the DAS. Channels correspond to locations at every 0.25 m along the fiber optic cable. Channel positions are correlated with depth by using the depth of water within the liner. Where the DAS fiber leaves the water, noise increases significantly (see 10 m depth and 7 m depth in FSE 9 and FSE 10, respectively). However, it is important to recall that the increase in the DAS signal noise is offset from the water level by one-half the gauge length. We originally attempted to locate fiber position by performing tap tests were the fiber entered the well, but these signals were difficult to discern when the data were later processed.

From previous logging and packer testing in these wells, hydraulically active fractures were known to be present in FSE 9 at 43 m depth and FSE 10 and 28 m depth (Johnson & Dunstan, 1998). These depths correspond well with the peak amplitudes in displacement measured by DAS, even though the signal is smeared by the effect of the gauge length. In FSE 10, the lower limit of displacement is very sharp because the lower gauge width of the sensing window corresponds closely with the depth of the liner (blue dotted line). Below this depth, the fiber optic cable is not mechanically coupled to the borehole wall, so no displacement is measured. The peak displacement in FSE 10 corresponds well with the known depth of the hydraulically stressed fracture or fracture zone, but the displacement is not symmetric about the fracture zone as might be expected from the laboratory experiments.

FSE 9 shows more complicated displacement profile. Like in FSE 10, the peak displacement corresponds well with a hydraulically stressed fracture zone. In addition to this known fracture zone at 43 m depth, however, there appears to be a second displacement peak at a depth of about 28 m. This displacement peak corresponds to a logged fracture set at 27.3 m below top of casing (Johnson & Dunstan, 1998). If this is a hydraulically stressed fracture zone, it was not detected in previous hydraulic testing and flow logging. Neither did it show signs of oxidation as did the lower fracture. It is likely, therefore, that this fracture does not flow to the borehole under natural gradient conditions. It is also possible that the deflection in displacement signal was due, not to hydraulic stressing of the fracture set, but a change in stiffness due to the flexure of the fracture set or even the lithologic boundary, which is coincident at that depth.

4. Conclusions

The DAS instrument tested is capable of measuring very minute displacements in fiber optic cable, so long as that displacement is dynamic. Although laboratory measurements have shown that large displacements can be measured with periods as long as one-half day (Becker & Coleman, 2019), this instrument is more reliable with periods of less than 1 hour in our experience. When displacement is dynamic, however, DAS is highly sensitive to geomechanical strain. Displacements of less than 1 nm were detected in our experiments with good signal to noise. As we have reported previously, head variations in less than 2 mm resulted in measurable displacement in FSE 10 (Becker, Ciervo, et al., 2017). Although much work remains before DAS can be used as reliable measure of hydraulic stress, these experiments demonstrated that DAS has potential for mapping hydraulic connectivity in bedrock systems.

DAS provides an opportunity to observe previously unobserved geomechanical responses in bedrock aquifers and reservoirs. The complex profile of displacement measured in both wells shows that hydraulic propping of a fracture did not result in a simple separation of parallel rock blocks. Such a relative movement

would have produced a displacement profile similar to that induced in our laboratory experiments (Figure 1), whereas the displacement profile measured in the boreholes was more complex. Similarly, the transient displacement matrix (Figure S4) reveals a dynamic propagation of displacement away from the stressed fractures. The shape of this displacement profile may help elucidate the complex interaction between channeled flow in fracture networks and the corresponding geomechanical response in the surrounding rock matrix. In our wells, there was no obvious influence of lithology on displacement, although the increase in displacement at 27.3 m depth in FSE 9 was coincident with a lithologic boundary. The rock in the well field is unlikely to vary appreciably in stiffness so fracture flexure is considered to be the more important influence on displacement.

Although we were able to measure the displacement of fractures in response to fluid pressure, deriving hydraulics from fracture displacement is not straightforward. Previous experiments in this well field suggest that water moves in a highly heterogeneous or "channeled" manner through the fracture network (Becker & Shapiro, 2000, 2003). Channeled groundwater flow is typically in fractured bedrock (Tsang & Neretnieks, 1998). One would expect that fluid pressure distributed through larger channels would produce greater normal force on the fracture and, therefore, result in larger displacement of fractures. Geomechanical displacement of a fracture is a function not only of fluid propagation but of coupled strain the bulk matrix (Murdoch & Germanovich, 2012). In some cases, this can cause a delay in fluid pressure propagation with respect to mechanical strain propagation (Vinci et al., 2015). Consequently, fluid pressure in the vicinity of the well bore may cause measurable displacement in a fracture intersecting a borehole but not result in appreciable flow to the borehole. To make full use of displacement profiles, geomechanical simulations may be necessary.

The hydraulic logging capability of DAS in bedrock is limited by the gauge length. For very sparsely separated fractures in long boreholes, a 10 m gauge length may not be an important limitation. In denser fracture networks or over shorter intervals, as is the case in these experiments, the moving sensing window tends to smear the displacement signal. Mathematically, the displacement profile is the result of a 10 m long "top hat" filter convolved with the true displacement. When the displacement occurs at a single point, the profile is easily interpreted. In bedrock, however, hydraulic stimulation will move the surrounding rock in a distributed manner. We have experimented with various methods of deconvolving the gauge window from the profile but have yet to find a reliable solution. We are currently calibrating forward models of geomechanical displacement to the DAS-measured displacement profile, but this too suffers from non-uniqueness. DAS systems using engineered sensing fiber are now commercially available that provide a 2 m gauge length with SNR better than the 10 m gauge length system used in this study. Shorter gauge lengths are expected to improve vertical resolution as DAS technology develops.

When considering the use of DAS in downhole applications, it is important to keep in mind that the fiber must be mechanically coupled to the formation to measure displacement. This can be accomplished using an overpressured liner, as was done in these experiments, or by grouting/cementing the cable into a borehole or outside a well casing as is done for seismic applications (Correa et al., 2019; Daley et al., 2013, 2016). Simply hanging a fiber in a well will not reliably produce any measure of formation displacement and, therefore, hydraulic response. Pressure changes in a water column will cause the fiber to compress radially, which may result in a measurable displacement (lengthening) of the fiber according the Poisson's ratio of the fiber glass. Our laboratory tests indicate that heads of about 10 cm or more are necessary to make a measurable displacement in the fiber (Becker, Coleman, et al., 2017), so it is not a very sensitive direct measurement of fluid pressure. In any case, variations in fluid pressure in an open wellbore are generally uninteresting in shallow wells.

The more fundamental limitation of using DAS as a hydraulic sensor is that displacement is an imperfect measurement of fluid pressure. Fracture normal stress and strain are related by a fracture "compliance," which is better defined in laboratories than in field situations. In addition, fiber displacement is measured in only one direction so fracture compliance may not be correctly quantified by DAS. In the circumstance where the fiber is oriented parallel to the fracture or fracture set, hydrualic propping may go undetected. Our previous analysis of the FSE 10 well data (Becker, Ciervo, et al., 2017) and the positive relationship between injection period and displacement in both FSE 9 and FSE 10 indicate, however, that DAS can provide at least a relative measure of hydraulic response. Such a relationship is not limited to consolidated

formations. Fluid stress in confined hydrostratigraphic units in alluvial aquifers, for example, should also show a relatively focused displacement in DAS displacement profiles.

The application of DAS to geologic and hydrogeologic problems is in its infancy. The instruments are still not widely available or cost-effective for most hydrologic applications. However, the same could have been said of fiber optic distributed temperature sensing (DTS) 25 years ago, and now DTS has become an indespensible tool for many hydrologic applications (Bense et al., 2016). Workshops are being convened at meetings to exchange experiences and inform potential users about the technology. The National Science Foundation recently established a Research Coordination Network (RCN) to help facilitate the development of DAS technology in Geosciences and Engineering (EAR 1948737). DAS is usually deployed for seismic observations rather than geomechnical observations, but low frequency signals in gas and oil fields are already being analyzed for hydraulic influences (Jin et al., 2019; Jin & Roy, 2017). Deployments of fiber intended to measure seismic signals or temperature, therefore, may find a new life for hydraulic or geomechanical sensing.

Data Availability Statement

Reduced (decimated) DAS data are available on the Geothermal Data Repository (http://gdr.openei.org/submissions/929). Example scripts for retrieving displacement amplitudes from DAS files are also provided onlie (http://gdr.openei.org/submissions/1220).

Acknowledgments
This research was funded by the Department of Energy Geothermal Technologies Program under Grant DE-EE0006763 and the National Science Foundation under Grant MRI-1920334. We are grateful for logistic support from the Hubbard Brook Experimental Forest and field assistance from Adam Hawkins and Matthew Cole.

References

Ajo-Franklin, J., Dou, S., Daley, T., Freifeld, B., Robertson, M., Ulrich, C., et al. (2017). *Time-lapse surface wave monitoring of permafrost thaw using distributed acoustic sensing and a permanent automated seismic source*. Paper presented at SEG Technical Program Expanded Abstracts 2017, Society of Exploration Geophysicists.

Barton, C. C., Camerlo, R. H., & Bailey, S. W. (1997). *Bedrock geologic map of the Hubbard Brook experimental forest and maps of fractures and geology in roadcuts along Interstate 93, Grafton County, New Hampshire, Miscellaneous Investigations Series Map I-2562*. Reston, VA: U.S. Geological Survey.

Becker, M. W., Ciervo, C., & Coleman, T. (2018a). A slimhole approach to measuring distributed hydromechanical strain in fractured geothermal reservoirs. In R. Horne (Ed.), *43rd Workshop on Geothermal Reservoir Engineering, SGP-TR-213*. Stanford, CA: Stanford University.

Becker, M. W., Ciervo, C., & Coleman, T. I. (2018b). *Laboratory testing of low-frequency strain measured by distributed acoustic sensing (DAS)* (pp. 4963–4966). Paper presented at SEG Technical Program Expanded Abstracts 2018, Society of Exploration Geophysicists.

Becker, M. W., Ciervo, C. C., Cole, M., Coleman, T. I., & Mondanos, M. (2017). Fracture hydromechanical response measured by fiber optic distributed acoustic sensing at milliHertz frequencies. *Geophysical Research Letters*, *44*, 7295–7302. https://doi.org/10.1002/2017GL073931

Becker, M. W., Cole, M., Ciervo, C., Coleman, T., & Mondanos, M. J. (2016). Measuring hydraulic connection in fractured bedrock with periodic hydraulic tests and distributed acoustic sensing. *Paper presented at 41st Workshop on Geothermal Reservoir Engineering*. Stanford, CA: Stanford University.

Becker, M. W., & Coleman, T. I. (2017). *Distributed Acoustic Sensing (DAS) data for periodic hydraulic tests [data set]*. https://doi.org/10.15121/1432544

Becker, M. W., & Coleman, T. I. (2019). Distributed acoustic sensing of strain at earth tide frequencies. *Sensors*, *19*(9), 1975. https://doi.org/10.3390/s19091975

Becker, M. W., Coleman, T. I., Ciervo, C. C., Cole, M., & Mondanos, M. (2017). Fluid pressure sensing with fiber-optic distributed acoustic sensing. *The Leading Edge*, *36*(12), 1018–1023. https://doi.org/10.1190/tle36121018.1

Becker, M. W., & Shapiro, A. M. (2000). Tracer transport in fractured crystalline rock: Evidence of nondiffusive breakthrough tailing. *Water Resources Research*, *36*(7), 1677–1686. https://doi.org/10.1029/2000wr900080

Becker, M. W., & Shapiro, A. M. (2003). Interpreting tracer breakthrough tailing from different forced-gradient tracer experiment configurations in fractured bedrock. *Water Resources Research*, *39*(1), 1024. https://doi.org/10.1029/2001WR001190

Bense, V. F., Read, T., Bour, O., Le Borgne, T., Coleman, T., Krause, S., et al. (2016). Distributed temperature sensing as a downhole tool in hydrogeology. *Water Resources Research*, *52*, 9259–9273. https://doi.org/10.1002/2016WR018869

Cannon, R. T., & Aminzadeh, F. (2013). *Distributed Acoustic Sensing: State of the art, SPE-163688-MS*. Society of Petroleum Engineers. https://doi.org/10.2118/163688-MS

Cherry, J. A., Parker, B. L., & Keller, C. (2007). A new depth-discrete multilevel monitoring approach for fractured rock. *Ground Water Monitoring & Remediation*, *27*(2), 57–70. https://doi.org/10.1111/j.1745-6592.2007.00137.x

Correa, J., Pevzner, R., Bona, A., Tertyshnikov, K., Freifeld, B., Robertson, M., & Daley, T. (2019). 3D vertical seismic profile acquired with distributed acoustic sensing on tubing installation: A case study from the CO2CRC Otway project. *Interpretation*, *7*(1), SA11–SA19. https://doi.org/10.1190/INT-2018-0086.1

Daley, T., Freifeld, B., Ajo-Franklin, J., Dou, S., Pevzner, R., Shulakova, V., et al. (2013). Field testing of fiber-optic distributed acoustic sensing (DAS) for subsurface seismic monitoring. *The Leading Edge*, *32*(6), 699–706. https://doi.org/10.1190/tle32060699.1

Daley, T. M., Miller, D. E., Dodds, K., Cook, P., & Freifeld, B. M. (2015). Field testing of modular borehole monitoring with simultaneous distributed acoustic sensing and geophone vertical seismic profiles at Citronelle, Alabama. *Geophysical Prospecting*, *64*, 1318–1334. https://doi.org/10.1111/1365-2478.12324

Daley, T. M., Miller, D. E., Dodds, K., Cook, P., & Freifeld, B. M. (2016). Field testing of modular borehole monitoring with simultaneous distributed acoustic sensing and geophone vertical seismic profiles at Citronelle, Alabama. *Geophysical Prospecting*, *64*(5), 1318–1334. https://doi.org/10.1111/1365-2478.12324

Ellefsen, K. J., Kibler, J. E., Hsieh, P. A., & Shapiro, A. M. (1998). *Crosswell seismic tomography at the USGS fractured rock research site; data collection, data processing, and tomograms (Open-File Report 98-510)*. Reston, VA: U.S. Geological Survey.

Hartog, A. H. (2017). *An introduction to distributed optical fibre sensors* (pp. 1–472). Boca Raton, FL: CRC Press. https://doi.org/10.1201/9781315119014

Hsieh, P. A., & Shapiro, A. M. (1996). Hydraulic characteristics of fractured bedrock underlying the FSE well field at the Mirror Lake Site, Grafton County, New Hampshire. In D. W. Morganwalp & D. A. Aronson (Eds.), *Proceedings of the Technical Meeting, U.S. Geological Survey Toxic Substances Hydrology Program*. Reston, VA: U.S. Geological Survey. Retrieved from https://hubbardbrook.org/hydraulic-characteristics-fractured-bedrock-underlying-fse-well-field-mirror-lake-site-grafton

Illman, W. A., Liu, X. Y., Takeuchi, S., Yeh, T. C. J., Ando, K., & Saegusa, H. (2009). Hydraulic tomography in fractured granite: Mizunami underground research site, Japan. *Water Resources Research*, *45*, W01406. https://doi.org/10.1029/2007WR006715

Jin, G., Mendoza, K., Roy, B., & Buswell, D. G. (2019). Machine learning-based fracture-hit detection algorithm using LFDAS signal. *The Leading Edge*, *38*(7), 520–524. https://doi.org/10.1190/tle38070520.1

Jin, G., & Roy, B. (2017). Hydraulic-fracture geometry characterization using low-frequency DAS signal. *The Leading Edge*, *36*(12), 975–980. https://doi.org/10.1190/tle36120975.1

Johnson, C. D., & Dunstan, A. H. (1998). *Lithology and fracture characterization from drilling investigations in the Mirror Lake area, Grafton County, New Hampshire, USGS Water-Resources Investigations Report Number 98-4183*. Reston, VA: U.S. Geological Survey. https://doi.org/10.3133/wri984183

Jousset, P., Reinsch, T., Ryberg, T., Blanck, H., Clarke, A., Aghayev, R., et al. (2018). Dynamic strain determination using fibre-optic cables allows imaging of seismological and structural features. *Nature Communications*, *9*(1), 2509. https://doi.org/10.1038/s41467-018-04860-y

Keller, C. E. (2016). *Method for air-coupled water level meter system, United States Patent Application Number 14/846243*.

Klepikova, M. V., Le Borgne, T., Bour, O., Gallagher, K., Hochreutener, R., & Lavenant, N. (2014). Passive temperature tomography experiments to characterize transmissivity and connectivity of preferential flow paths in fractured media. *Journal of Hydrology*, *512*, 549–562. https://doi.org/10.1016/j.jhydrol.2014.03.018

Li, M., Wang, H., & Tao, G. (2015). Current and future applications of distributed acoustic sensing as a new reservoir geophysics tool. *Open Petroleum Engineering Journal*, *8*(1), 272–281. https://doi.org/10.2174/1874834101508010272

Lindsey, N. J., Martin, E. R., Dreger, D. S., Freifeld, B., Cole, S., James, S. R., et al. (2017). Fiber-optic network observations of earthquake wavefields. *Geophysical Research Letters*, *44*(23), 11,792–11,799. https://doi.org/10.1002/2017gl075722

Lindsey, N. J., Rademacher, H., & Ajo-Franklin, J. B. (2020). On the broadband instrument response of fiber-optic DAS arrays. *Journal of Geophysical Research: Solid Earth*, *125*, e2019JB018145. https://doi.org/10.1029/2019JB018145

Lyons, R. (2011). Reducing FFT scalloping loss errors without multiplication. *IEEE Signal Processing Magazine*, *28*(2), 112–116. https://doi.org/10.1109/msp.2010.939845

Munn, J. D., Coleman, T. I., Parker, B. L., Mondanos, M. J., & Chalari, A. (2017). Novel cable coupling technique for improved shallow distributed acoustic sensor VSPs. *Journal of Applied Geophysics*, *138*, 72–79. https://doi.org/10.1016/j.jappgeo.2017.01.007

Murdoch, L. C., & Germanovich, L. N. (2012). Storage change in a flat-lying fracture during well tests. *Water Resources Research*, *48*, W12528. https://doi.org/10.1029/2011WR011571

National Academies of Sciences and Medicine (2015). *Characterization, modeling, monitoring, and remediation of fractured rock*. Washington, DC: The National Academies Press. https://doi.org/10.17226/21742

National Research Council (1996). *Rock fractures and fluid flow: Contemporary understanding and applications* (p. 551). Washington, DC: National Academy Press. https://doi.org/10.17226/2309

Paillet, F. L. (1993). Using borehole geophysics and cross-borehole flow testing to define hydraulic connections between fracture zones in bedrock aquifers. *Journal of Applied Geophysics*, *30*(4), 261–279. https://doi.org/10.1016/0926-9851(93)90036-x

Parker, T., Shatalin, S., & Farhadiroushan, M. (2014). Distributed acoustic sensing; a new tool for seismic applications. *First Break*, *32*(2). https://doi.org/10.3997/1365-2397.2013034

Paulsson, B. N. P., Toko, J. L., Thornburg, J. A., Slopko, F., & He, R. (2014). Development and test of a 300°C fiber optic borehole seismic system (SGP-TR-202). *Paper presented at Thirty-Ninth Workshop on Geothermal Reservoir Engineering*. Stanford, CA: Stanford University.

Rasmussen, T. C., Haborak, K. G., & Young, M. H. (2003). Estimating aquifer hydraulic properties using sinusoidal pumping at the Savannah River site, South Carolina, USA. *Hydrogeology Journal*, *11*(4), 466–482. https://doi.org/10.1007/s10040-003-0255-7

Richter, P., Parker, T., Woerpel, C., Wu, Y., Rufino, R., & Farhadiroushan, M. (2019). Hydraulic fracture monitoring and optimization in unconventional completions using a high-resolution engineered fibre-optic Distributed Acoustic Sensor. *First Break*, *37*(4), 63–68. https://doi.org/10.3997/1365-2397.n0021

Schenato, L. (2017). A review of distributed fibre optic sensors for geo-hydrological applications. *Applied Science-Basel*, *7*(9), 896. https://doi.org/10.3390/APP7090896

Schuite, J., Longuevergne, L., Bour, O., Guihéneuf, N., Becker, M. W., Cole, M., et al. (2017). Combining periodic hydraulic tests and surface tilt measurements to explore in situ fracture hydromechanics. *Journal of Geophysical Research: Solid Earth*, *122*, 6046–6066. https://doi.org/10.1002/2017JB014045

Shapiro, A. M. (2001). Effective matrix diffusion in kilometer-scale transport in fractured crystalline rock. *Water Resources Research*, *37*(3), 507–522. https://doi.org/10.1029/2000WR900301

Shapiro, A. M., Hsieh, P. A., & Winter, T. C. (1995). *The Mirror Lake fractured-rock research site; a multidisciplinary research effort in characterizing ground-water flow and chemical transport in fractured rock*. Reston, VA: Fact Sheet, U.S. Geological Survey.

Tsang, C. F., & Neretnieks, I. (1998). Flow channeling in heterogeneous fractured rocks. *Reviews of Geophysics*, *36*(2), 275–298. https://doi.org/10.1029/97RG03319

Vinci, C., Steeb, H., & Renner, J. (2015). The imprint of hydro-mechanics of fractures in periodic pumping tests. *Geophysical Journal International*, *202*, 1613–1626. https://doi.org/10.1093/gji/ggv247